

VV precision predictions – Vector boson pair production at hadron colliders at NNLO QCD

Stefan Kallweit¹

based on work with: F. Cascioli^b, T. Gehrmann^{bc}, M. Grazzini^{a-h}, P. Maierhöfer^{bc}, A. v. Manteuffel^{bc}, S. Pozzorini^{bch}, D. Rathlev^{a-h}, L. Tancredi^{bc}, A. Torre^a, E. Weihs^b, M. Wiesemann^{egh}

^h arXiv:1605.02716 [hep-ph] ^g arXiv:1604.08576 [hep-ph]

^f Phys.Lett. B750 (2015) 407-410 [arXiv:1507.06257 [hep-ph]]

^e JHEP 1508 (2015) 154 [arXiv:1507.02565 [hep-ph]]

^d JHEP 1507 (2015) 085 [arXiv:1504.01330 [hep-ph]]

^c Phys.Rev.Lett. 113 (2014) 21, 212001 [arXiv:1408.5243 [hep-ph]]

^b Phys.Lett. B735 (2014) 311-313 [arXiv:1405.2219 [hep-ph]]

^a Phys.Lett. B731 (2014) 204-207 [arXiv:1309.7000 [hep-ph]]

¹University of Mainz

Fourth Annual Large Hadron Collider Physics Conference (LHCPh2016)
Lund, Sweden, June 13 – 18, 2016



Outline

1 Introduction

- Motivation for NNLO QCD accuracy in VV production

2 Calculation of NNLO QCD cross sections in the MATRIX framework

- The MATRIX framework in a nutshell

3 Numerical results at NNLO QCD

- NNLO QCD results for $pp \rightarrow W^\pm Z (\rightarrow 3\ell\nu) + X$
- NNLO QCD results for $pp (\rightarrow W^+W^-) \rightarrow 2\ell 2\nu + X$
- NNLO QCD results for $pp (\rightarrow ZZ) \rightarrow 4\ell + X$

4 Conclusions & Outlook

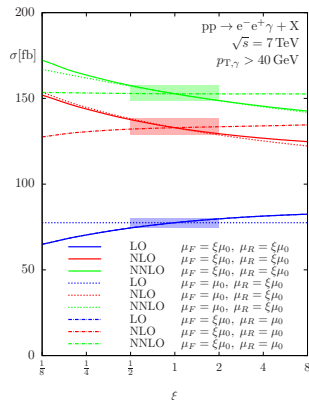
Importance of going beyond NLO in QCD for VV production

Fully exclusive NNLO QCD calculations desirable for several reasons

- Experimental accuracy has significantly increased.
- A reduction of the unphysical dependence on factorization and renormalization scales — and in particular reliability of the remaining scale-variation uncertainty as an estimate for missing higher orders — is expected at NNLO.
- In many process classes, all partonic channels are included only from NNLO on.
- In some phase-space regions, NLO is the first non-vanishing order.
- Jets are treated more realistically.

NLO EW corrections could contribute at the same order of magnitude, at least by naive counting of coupling constants, $\alpha_s^2 \approx \alpha$.

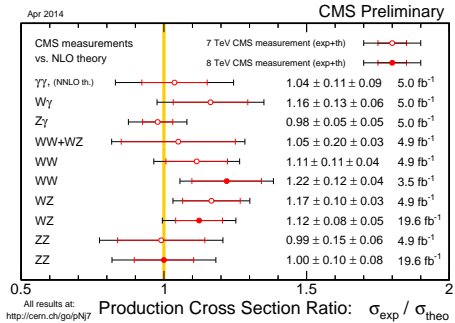
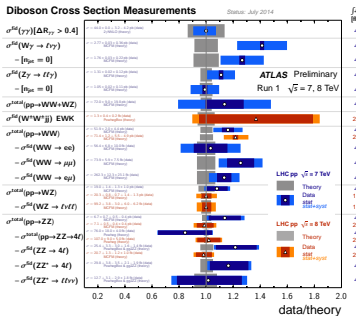
Leading N³LO QCD corrections can be significant (namely the gg channel, which enters only at NNLO).



Data-theory comparison for VV cross sections — status mid of 2014

Importance of VV production (with leptonic decays) at NNLO QCD

- Important Standard Model test → trilinear gauge-boson couplings.
- Background for Higgs analyses and BSM searches.
- Some **moderate excesses ($\approx 2\sigma$)** in experimental data compared to **NLO** prediction, e.g. $W\gamma$ (ATLAS, 7 TeV), WW (ATLAS, 8 TeV; milder excess also seen at CMS).



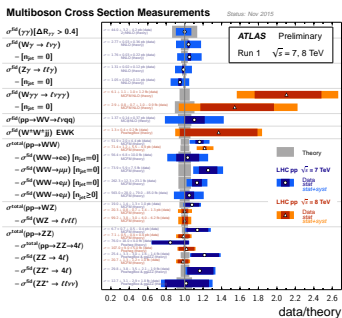
[ATLAS collaboration, July 2014]

[CMS collaboration, April 2014]

Data-theory comparison for VV cross sections — status end of 2015

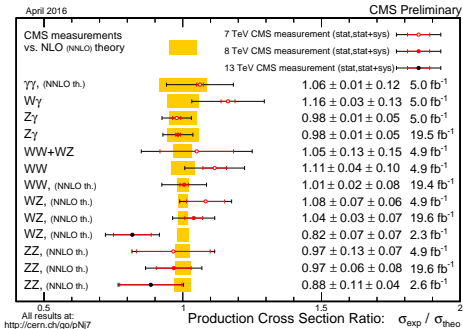
Importance of VV production (with leptonic decays) at NNLO QCD

- Important Standard Model test → trilinear gauge-boson couplings.
- Background for Higgs analyses and BSM searches.
- Inclusion of NNLO QCD corrections tends to resolve these moderate excesses
(also important: extrapolation from fiducial region to inclusive prediction (WW)).



| | $\int d\zeta dt$ [fb $^{-1}$] | Reference |
|---|-----------------------------------|---|
| $\sigma^{\text{fid}}(\gamma\gamma \rightarrow \Delta R_{\gamma\gamma} > 0.4)$ | 4.9 | JHEP 01, 086 (2013) |
| $\sigma^{\text{fid}}(W\gamma \rightarrow l\nu\gamma)$ - $[n_{\text{jet}} = 0]$ | 4.6 | PRD 87, 112003 (2013); arXiv:1407.1618 [hep-ph] |
| $\sigma^{\text{fid}}(Z\gamma \rightarrow ll\gamma)$ - $[n_{\text{jet}} = 0]$ | 4.6 | PRD 87, 112003 (2013) |
| $\sigma^{\text{fid}}(W\gamma\gamma \rightarrow ll\gamma\gamma)$ - $[n_{\text{jet}} = 0]$ | 20.3 | arXiv:1503.03240 [hep-ph] |
| $\sigma^{\text{fid}}(pp \rightarrow VV \rightarrow l\nu qq)$ | 20.3 | arXiv:1503.03240 [hep-ph] |
| $\sigma^{\text{fid}}(WW^{\pm})$ EWK | 4.6 | JHEP 01, 049 (2013) |
| $\sigma^{\text{total}}(pp \rightarrow WW)$ | 20.3 | PRD 113, 141803 (2014) |
| $\sigma^{\text{total}}(pp \rightarrow WW)$ - $\sigma^{\text{fid}}(WW \rightarrow ee) [n_{\text{jet}} = 0]$ | 20.3 | ATLAS-CDF-2014-033 |
| $\sigma^{\text{total}}(WW \rightarrow \mu\mu) [n_{\text{jet}} = 0]$ | 4.6 | PRD 87, 112001 (2013) |
| $\sigma^{\text{total}}(WW \rightarrow ee) [n_{\text{jet}} \geq 0]$ | 4.6 | PRD 87, 112001 (2013) |
| $\sigma^{\text{total}}(WW \rightarrow \mu\mu) [n_{\text{jet}} \geq 0]$ | 4.6 | PRD 87, 112001 (2013) |
| $\sigma^{\text{total}}(pp \rightarrow WZ)$ | 4.6 | arXiv:1407.0273 [hep-ph] |
| $\sigma^{\text{total}}(WZ \rightarrow ll\ell\ell)$ | 13.0 | EPJC 73, 2773 (2013); ATLAS-CDF-2013-021 |
| $\sigma^{\text{total}}(pp \rightarrow ZZ)$ | 13.0 | ATLAS-CDF-2013-021 |
| $\sigma^{\text{total}}(pp \rightarrow ZZ + 4\ell)$ | 20.3 | arXiv:1403.0657 [hep-ph] |
| $\sigma^{\text{total}}(ZZ \rightarrow 4\ell)$ | 20.3 | JHEP 03, 128 (2013) |
| $\sigma^{\text{total}}(ZZ^{\pm} \rightarrow 4\ell)$ | 4.6 | JHEP 03, 128 (2013) |
| $\sigma^{\text{total}}(ZZ^{\pm} \rightarrow ll\nu\nu)$ | 4.6 | JHEP 03, 128 (2013) |

[ATLAS collaboration, November 2015]



[CMS collaboration, April 2016]

The MATRIX framework for automated NNLO+NNLL calculations

[Grazzini, SK, Rathlev, Wiesemann]

Amplitudes

OPENLOOPS
(COLLIER, CUTTOOLS, ...)

Dedicated 2-loop codes
(VVAMP, GiNAC, TDHPL, ...)

MUNICH
MULTI-channel Integrator at Swiss (CH) precision

q_T subtraction \Leftrightarrow q_T resummation

NNLO

NNLL

MATRIX

MUNICH Automates q_T subtraction
and Resummation to Integrate X-sections.

Processes available at NNLO QCD within the MATRIX framework

- $\text{pp} \rightarrow \mathbf{H} + \text{X}$ ($m_t \rightarrow \infty$)
 - agreement with **HNNLO**
 [Catani, Grazzini (2007); Grazzini (2008), Grazzini, Sargsyan (2013)]

- $\text{pp} (\rightarrow \mathbf{Z}) \rightarrow \ell^-\ell^+ + \text{X}$
 - agreement with **ZWPROM** (on-shell Z)
 [Hamberg, van Neerven, Matsuura (1991 & 2002)]
 - agreement with **DYNNLO**
 [Catani, Grazzini (2007); Catani, Cieri, Ferrera, de Florian, Grazzini (2009)]

- $\text{pp} (\rightarrow \mathbf{W}^\pm) \rightarrow \ell\nu + \text{X}$

- $\text{pp} \rightarrow \gamma\gamma + \text{X}$
 - agreement with **2GAMMANNLO**
 [Catani, Cieri, Ferrera, de Florian, Grazzini (2011)]
 (updated version from Nov 2015)

- $\text{pp} (\rightarrow \mathbf{Z}\gamma) \rightarrow \ell^-\ell^+\gamma/\nu\bar{\nu}\gamma + \text{X}$

- $\text{pp} (\rightarrow \mathbf{W}^\pm\gamma) \rightarrow \ell\nu\gamma + \text{X}$

- $\text{pp} (\rightarrow \mathbf{ZZ}) \rightarrow \ell^-\ell^+\ell^-\ell^+/\ell^-\ell^+\ell^-\ell^+/\ell^-\ell^+\nu'\bar{\nu}'/\ell^-\ell^+\nu\bar{\nu} + \text{X}$

- $\text{pp} (\rightarrow \mathbf{W^+W^-}) \rightarrow \ell^+\nu\ell^-\bar{\nu}'/\ell^+\nu\ell^-\bar{\nu} + \text{X}$

- $\text{pp} (\rightarrow \mathbf{W}^\pm\mathbf{Z}) \rightarrow \ell\nu\ell^-\ell^+/\ell\nu\ell^-\ell^+ + \text{X}$

NLO EW corrections

are implemented in
MUNICH + **OPENLOOPS**
 in a fully automated way!

→ They can be easily
 made available within
MATRIX
 for all (off-shell)
V and **VV'** processes.

NNLO QCD results for $pp (\rightarrow W^\pm Z) \rightarrow 3\ell\nu + X$

$$pp \rightarrow W^+ Z + X$$

$$pp \rightarrow W^- Z + X$$

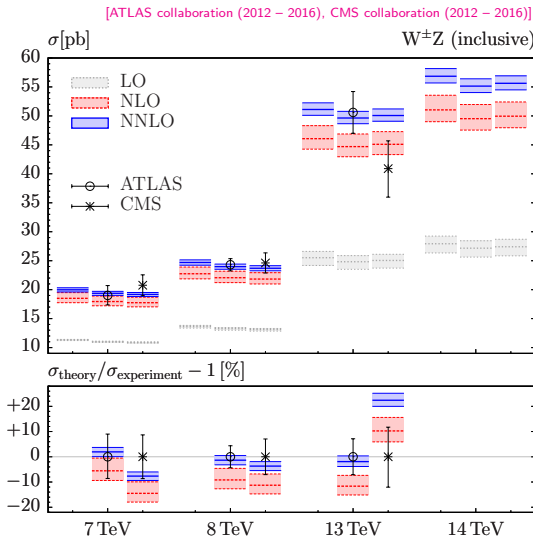
$$pp (\rightarrow W^+ Z) \rightarrow \ell^- \ell^+ \ell'^+ \nu_{\ell'} + X$$

$$pp (\rightarrow W^- Z) \rightarrow \ell^- \ell'^- \ell^+ \bar{\nu}_{\ell'} + X$$

$$pp (\rightarrow W^+ Z) \rightarrow \ell^- \ell^+ \ell^+ \nu_\ell + X$$

$$pp (\rightarrow W^- Z) \rightarrow \ell^- \ell^- \ell^+ \bar{\nu}_\ell + X$$

Inclusive WZ cross sections for relevant LHC energies



- MATRIX results with NNPDF3.0 PDF sets.

- **on-shell (left):** $m_{\ell\ell/\ell\nu} = m_Z/W$
- **ATLAS (center):**
 $66 \text{ GeV} < m_{\ell\ell} < 116 \text{ GeV}$
- **CMS (right):**
 $71 \text{ GeV} < m_{\ell\ell} < 111 \text{ GeV}$
(7 and 8 TeV)
 $60 \text{ GeV} < m_{\ell\ell} < 120 \text{ GeV}$
(13 and 14 TeV)
- **NNLO scale variation $\approx \pm 2\%$ with $\mu_0 = (M_W + M_Z)/2$.**

$$\left(\frac{\mu_0}{2} \leq \mu_R, \mu_F \leq 2\mu_0 \right)$$

$$\left(\frac{1}{2} \leq \mu_R/\mu_F \leq 2 \right)$$
- **Large NLO corrections due to approximate radiation zero, which is broken beyond LO.**
- **NNLO/NLO ranges from 8% to 11% (7 TeV to 14 TeV).**
- **No NLO EW included.**

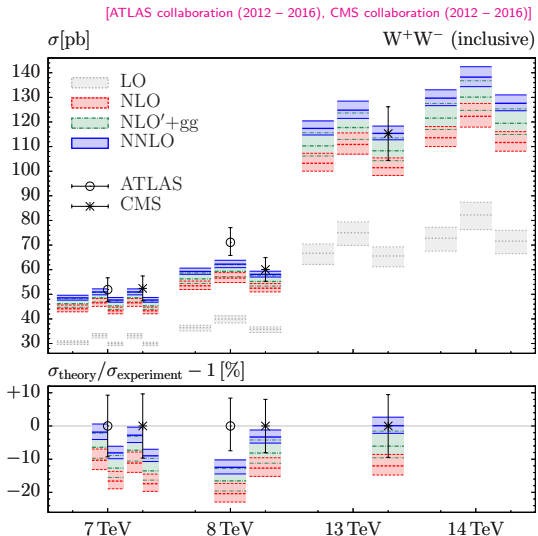
NNLO QCD results for $pp \rightarrow W^+W^- \rightarrow 2\ell 2\nu + X$

$$pp \rightarrow W^+ W^- + X$$

$$pp \rightarrow W^+ W^- \rightarrow \ell^- \ell'^+ \nu_{\ell'} \bar{\nu}_{\ell} + X$$

$$pp \rightarrow W^+ W^- / ZZ \rightarrow \ell^- \ell^+ \nu_{\ell} \bar{\nu}_{\ell} + X$$

Inclusive WW cross sections for relevant LHC energies



- **on-shell (left):** $m_{\ell\nu} = m_W$
ATLAS (center): 8, 13, 14 TeV:
 $H \rightarrow WW^*$ included
CMS (right): 8, 13, 14 TeV:
 $H \rightarrow WW^*$ not included
ATLAS and **CMS**: 7 TeV:
Predictions shown with (left) and without (right) $H \rightarrow WW^*$
- **NNLO scale variation $\approx \pm 3\%$.**
 $(M_W/2 \leq \mu_R, \mu_F \leq 2M_W)$
 $1/2 \leq \mu_R/\mu_F \leq 2$
- **NNLO/NLO ranges from 9% to 12% (7 TeV to 14 TeV).**
- Loop-induced gg channel makes for about 35% of NNLO effect.
- No NLO EW or NLO QCD to gg-fusion channel included.

- MATRIX results with NNPDF3.0 PDF sets.

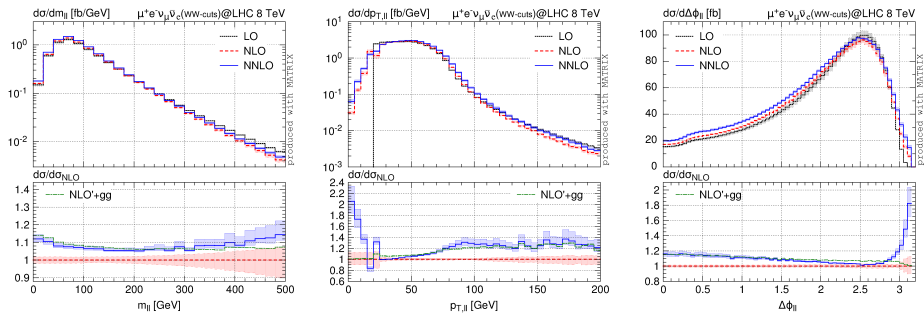
Fiducial off-shell cross sections for $pp \rightarrow W^+W^- \rightarrow 2\ell 2\nu + X$

Setup motivated by the ATLAS analysis @ 8 TeV [ATLAS collaboration (2014 & 2016)]

| \sqrt{s} | $\sigma_{\text{fiducial}}(W^+W^- \text{-cuts}) [\text{fb}]$ | | $\sigma/\sigma_{\text{NLO}} - 1$ | |
|------------|---|--------------------------------|----------------------------------|--------|
| | 8 TeV | 13 TeV | 8 TeV | 13 TeV |
| LO | 147.23 (2) $^{+3.4\%}_{-4.4\%}$ | 233.04(2) $^{+6.6\%}_{-7.6\%}$ | -3.8% | - 1.3% |
| NLO | 153.07 (2) $^{+1.9\%}_{-1.6\%}$ | 236.19(2) $^{+2.8\%}_{-2.4\%}$ | 0 | 0 |
| NLO' | 156.71 (3) $^{+1.8\%}_{-1.4\%}$ | 243.82(4) $^{+2.6\%}_{-2.2\%}$ | +2.4% | + 3.2% |
| NLO' +gg | 166.41 (3) $^{+1.3\%}_{-1.3\%}$ | 267.31(4) $^{+1.5\%}_{-2.1\%}$ | +8.7% | +13.2% |
| NNLO | 164.16(13) $^{+1.3\%}_{-0.8\%}$ | 261.5(2) $^{+1.9\%}_{-1.2\%}$ | +7.2% | +10.7% |

- Results refer to only one different-flavour channel: $pp \rightarrow e^- \mu^+ \nu_\mu \bar{\nu}_e + X$
- Event selection imposes a jet veto, so usual scale variation most likely underestimates missing higher-order corrections.
- NLO corrections amount to about +4% (+1%) wrt. LO result at 8 (13) TeV.
- NNLO corrections amount to about +7% (+10%) wrt. NLO result at 8 (13) TeV.
- The positive impact of the NNLO corrections is entirely due to the loop-induced gg contribution, which is about +6% (+10%) wrt. NLO result at 8 (13) TeV.
 ↵ $\mathcal{O}(\alpha_s^2)$ corrections to $q\bar{q}$ are negative and amount to roughly -2% (-3%).

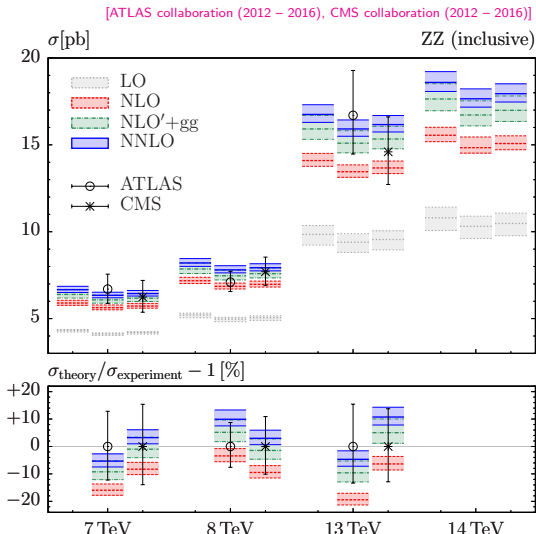
Distributions for $pp \rightarrow WW \rightarrow 2\ell 2\nu + X$ at NNLO QCD



- NLO and NNLO scale-variation bands typically do not overlap.
↪ The loop-induced gg contribution dominates the NNLO corrections.
- By and large the $NLO' + gg$ approximates the full NNLO prediction very well.
- However, shape distortions of up to 10% result from genuine NNLO corrections.
- In phase-space regions that imply the presence of QCD radiation, the loop-induced gg contribution cannot approximate the shapes of full NNLO corrections.

NNLO QCD results for $pp \rightarrow ZZ \rightarrow 4\ell + X$
$$pp \rightarrow Z Z + X$$
$$pp (\rightarrow ZZ) \rightarrow \ell^- \ell^+ \ell'^- \ell'^+ + X$$
$$pp (\rightarrow ZZ) \rightarrow \ell^- \ell^+ \ell^- \ell^+ + X$$
$$pp (\rightarrow ZZ) \rightarrow \ell^- \ell^+ \nu_{\ell'} \bar{\nu}_{\ell'} + X$$
$$pp (\rightarrow W^+W^-/ZZ) \rightarrow \ell^- \ell^+ \nu_\ell \bar{\nu}_\ell + X$$

Inclusive ZZ cross sections for relevant LHC energies



- **on-shell (left):** $m_{\ell\ell} = m_Z$
- **ATLAS (center):**
 $66 \text{ GeV} < m_{\ell\ell} < 116 \text{ GeV}$
- **CMS (right):**
 $60 \text{ GeV} < m_{\ell\ell} < 120 \text{ GeV}$
- **NNLO scale variation $\approx \pm 3\%$.**

$$\left(M_Z/2 \leq \mu_R, \mu_F \leq 2M_Z \right)$$

$$\left(1/2 \leq \mu_R/\mu_F \leq 2 \right)$$
- NNLO/NLO ranges from 12% to 17% (7 TeV to 14 TeV).
- Loop-induced gg channel makes for about 60% of NNLO effect.
- No NLO EW or NLO QCD to gg-fusion channel included.

- MATRIX results with NNPDF3.0 PDF sets.

Fiducial off-shell cross sections for $pp \rightarrow ZZ \rightarrow 4\ell + X$

Setup adapted to the ATLAS analysis @ 8 TeV [ATLAS collaboration (2013)]

| channel | σ_{LO} [fb] | σ_{NLO} [fb] | σ_{NNLO} [fb] | σ_{ATLAS} [fb] |
|---------------------------|------------------------------|------------------------------|------------------------------|---|
| $e^+ e^- e^+ e^-$ | $3.547(1)^{+2.9\%}_{-3.9\%}$ | $5.047(1)^{+2.8\%}_{-2.3\%}$ | $5.79(2)^{+3.4\%}_{-2.6\%}$ | $4.6^{+0.8}_{-0.7}(\text{stat})^{+0.4}_{-0.4}(\text{syst})^{+0.1}_{-0.1}(\text{lumi})$ |
| $\mu^+ \mu^- \mu^+ \mu^-$ | | | | $5.0^{+0.6}_{-0.5}(\text{stat})^{+0.2}_{-0.2}(\text{syst})^{+0.2}_{-0.2}(\text{lumi})$ |
| $e^+ e^- \mu^+ \mu^-$ | $6.950(1)^{+2.9\%}_{-3.9\%}$ | $9.864(2)^{+2.8\%}_{-2.3\%}$ | $11.31(2)^{+3.2\%}_{-2.5\%}$ | $11.1^{+1.0}_{-0.9}(\text{stat})^{+0.5}_{-0.5}(\text{syst})^{+0.3}_{-0.3}(\text{lumi})$ |

- Agreement significantly improved in different-flavour channel.
- Worse agreement in same-flavour channels, but still consistent at the $\approx 1\sigma$ level.

Setup adapted to the ATLAS analysis @ 13 TeV [ATLAS collaboration (2015)]

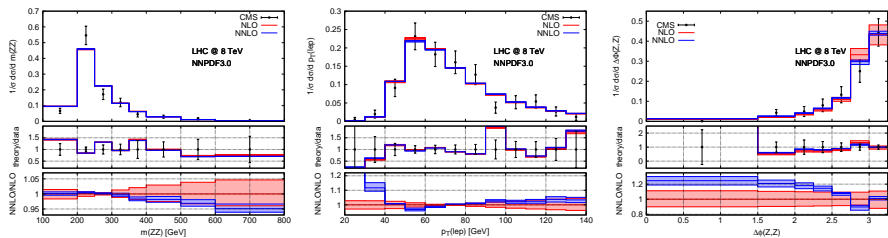
| channel | σ_{LO} [fb] | σ_{NLO} [fb] | σ_{NNLO} [fb] | σ_{ATLAS} [fb] |
|---------------------------|---------------------------|----------------------------|-----------------------------|---|
| $e^+ e^- e^+ e^-$ | $5.007(1)^{+4\%}_{-5\%}$ | $6.157(1)^{+2\%}_{-2\%}$ | $7.14(2)^{+2\%}_{-2\%}$ | $8.4^{+2.4}_{-2.0}(\text{stat})^{+0.4}_{-0.2}(\text{syst})^{+0.5}_{-0.3}(\text{lumi})$ |
| $\mu^+ \mu^- \mu^+ \mu^-$ | | | | $6.8^{+1.8}_{-1.5}(\text{stat})^{+0.3}_{-0.3}(\text{syst})^{+0.4}_{-0.3}(\text{lumi})$ |
| $e^+ e^- \mu^+ \mu^-$ | $9.906(1)^{+4\%}_{-5\%}$ | $12.171(2)^{+2\%}_{-2\%}$ | $14.19(2)^{+2\%}_{-2\%}$ | $14.7^{+2.9}_{-2.5}(\text{stat})^{+0.6}_{-0.4}(\text{syst})^{+0.9}_{-0.6}(\text{lumi})$ |

- Agreement improved at NNLO in all channels within quite large (statistical) errors.

Normalized distributions for off-shell $pp \rightarrow ZZ \rightarrow 4\ell + X$

Setup adapted to the CMS analysis @ 8 TeV [CMS collaboration (2015)]

| channel | $\sigma_{\text{LO}} [\text{fb}]$ | $\sigma_{\text{NLO}} [\text{fb}]$ | $\sigma_{\text{NNLO}} [\text{fb}]$ |
|---------------------------|----------------------------------|-----------------------------------|------------------------------------|
| $e^+ e^- e^+ e^-$ | $3.149(1)^{+3.0\%}_{-4.0\%}$ | $4.493(1)^{+2.8\%}_{-2.3\%}$ | $5.16(1)^{+3.3\%}_{-2.6\%}$ |
| $\mu^+ \mu^- \mu^+ \mu^-$ | $2.973(1)^{+3.1\%}_{-4.1\%}$ | $4.255(1)^{+2.8\%}_{-2.3\%}$ | $4.90(1)^{+3.4\%}_{-2.6\%}$ |
| $e^+ e^- \mu^+ \mu^-$ | $6.179(1)^{+3.1\%}_{-4.0\%}$ | $8.822(1)^{+2.8\%}_{-2.3\%}$ | $10.15(2)^{+3.3\%}_{-2.6\%}$ |



- $m(ZZ)$ and p_T^{lept} distributions: NNLO effect on shapes dominated by gg contribution, no significant NNLO impact on the data agreement.
- $\Delta\phi(ZZ)$ distribution: Shape agreement improves at NNLO ($\Delta\phi(ZZ) = \pi$ at LO).

Corrections to ZZ/WW (WZ) production beyond NNLO QCD

Remaining QCD uncertainty expected to be dominated by **gg-fusion contribution**:

- Two-loop amplitudes for $gg \rightarrow VV'$ are available from two independent calculations.
[Caola, Henn, Melnikov, Smirnov, Smirnov (2015); von Manteuffel, Tancredi (2015)]
- Recently, (part of) the NLO QCD corrections to $gg \rightarrow ZZ/W^+W^-$ were calculated.
[Caola, Melnikov, Röntsch, Tancredi (2015 & 2015)]

(NLO wrt. gg-fusion process, but N^3LO wrt. $q\bar{q}$ annihilation process)

↪ Impact wrt. NLO QCD $q\bar{q}$ prediction (setup of the NNLO QCD calculation):

$$ZZ: \approx +6\% \text{ (+12\%} \rightarrow +18\%) \quad WW: \approx +2\% \text{ (+9\%} \rightarrow +11\%) \quad (\sqrt{s} = 8 \text{ TeV})$$

NLO EW corrections are known (at least in approximations).

[Baglio, Ninh, Weber (2013)]; [Bierweiler, Kasprzik, Kühn (2013)]; Billoni, Dittmaier, Jäger, Speckner (2013);
[Biedermann, Denner, Dittmaier, Hofer, Jäger (2016)], [Biedermann, Billoni, Denner, Dittmaier, Hofer, Jäger, Salfelder (2016)]

↪ Corrections wrt. the inclusive (LO) cross section:

$$ZZ: \delta_{\text{NLO EW}} \approx -4\% \quad WW: \delta_{\text{NLO EW}} \approx -0.4\% \quad (\sqrt{s} = 8 \text{ TeV})$$

$$\delta_{\text{LO } \gamma\gamma} \approx +1\%$$

$$WZ: \delta_{\text{NLO EW}} \approx -1.3\%$$

- Typical tens of per cent corrections at high transverse momenta.

↪ **Both NLO QCD to gg and NLO EW corrections can be quantitatively relevant**, also at the level of inclusive cross sections, but happen to partially cancel.

Conclusions

MATRIX – an automated framework to perform fully differential NNLO (+NNLL) QCD computations for colourless final-state production – introduced, which is based on

- the **MUNICH** Monte Carlo integrator,
- the q_T subtraction (+resummation) method,
- **OPENLOOPSS** and dedicated 2-loop amplitudes.

NNLO QCD results calculated in the MATRIX framework

- Fully differential results for $pp \rightarrow V\gamma \rightarrow l\ell\gamma/\ell\nu\gamma/\nu\nu\gamma + X$
- Inclusive and fully differential results for $pp \rightarrow ZZ \rightarrow 4\ell + X$
 - NNLO/NLO (inclusive): **12% to 17%** (7 TeV to 14 TeV) ($\approx 60\%$ from gg).
- Inclusive and fully differential cross sections for $pp \rightarrow W^+W^- \rightarrow 2\ell 2\nu + X$
 - NNLO/NLO (inclusive): **9% to 12%** (7 TeV to 14 TeV) ($\approx 35\%$ from gg).
 - Different situation with jet-veto: gg dominates, $q\bar{q}$ slightly negative.
- Inclusive cross sections for $pp \rightarrow W^\pm Z \rightarrow 3\ell\nu + X$
 - NNLO/NLO (inclusive): **8% to 11%** (7 TeV to 14 TeV).

→ Improved agreement between data and theory by NNLO prediction.

Outlook

- More phenomenological studies on VV processes
 - Planned extensions of the MATRIX framework
 - Combination with NLO EW corrections (available in MUNICH+OPENLOOPS).
 - Implementation of gg-induced processes (leading $N^3\text{LO}$).
 - Simultaneous studies on pdf uncertainties, ...

- First step done:

Private beta version of the program MATRIX for selected ATLAS/CMS colleagues

- **Next step:**

Public version of
the program MATRIX

Overview

The figure consists of a 4x5 grid of slides, each containing a title, a brief description, and a plot or table. The slides are numbered 01 through 20.

- 01:** VBF precision predictions – Vector boson pair production at hadron colliders at NNLO QCD
- 02:** Outlines
- 03:** Importance of going beyond NLO in QCD for VV production
- 04:** Data-theory comparison for VV cross sections – status end of 2014
- 05:** Data-theory comparison for VV cross sections – status end of 2014
- 06:** The MATRIX framework for automated NLO+NNLL calculations
- 07:** Precision available at NNLO-QCD within the MATRIX framework
- 08:** NNLO-QCD results for $\langle p_T \rangle = W/Z \rangle \rightarrow l\nu + X$
- 09:** Inclusive WZ cross sections for relevant LHC energies
- 10:** NNLO QCD results for $\langle p_T \rangle = W/W' \rangle \rightarrow l\bar{l} + X$
- 11:** Inclusive WW cross sections for relevant LHC energies
- 12:** Total off-shell cross sections for $\langle p_T \rangle = W/W' \rangle \rightarrow 2l\nu + X$
- 13:** Distributions for $\langle p_T \rangle = W/W' \rangle \rightarrow 2l\nu + X$ at NNLO QCD
- 14:** NNLO QCD results for $\langle p_T \rangle = Z Z \rangle \rightarrow l\bar{l} + X$
- 15:** Inclusive ZZ cross sections for relevant LHC energies
- 16:** Total off-shell cross sections for $\langle p_T \rangle = Z Z \rangle \rightarrow 4l + X$
- 17:** Normalized distributions for off-shell $\langle p_T \rangle = Z Z \rangle \rightarrow l\bar{l} + X$
- 18:** Corrections to ZZ, WW (WZ) production beyond NNLO QCD
- 19:** Conclusions
- 20:** Outlook

Backup slides

External ingredients: amplitudes applied in the calculation

1-loop amplitudes with OPENLOOPS [Cascioli, Maierhöfer, Pozzorini (2011); Cascioli, Lindert, Maierhöfer, Pozzorini (2014)]

- All tree and (squared) one-loop amplitudes (including colour/helicity correlations)
- Fully automated compact and fast numerical code for any SM process (QCD+EW)
- Tensor reduction by means of the COLLIER library [Denner, Dittmaier, Hofer (2014)]
 - Numerically stable Denner–Dittmaier reduction methods [Denner, Dittmaier (2002 & 2005)]
 - Scalar integrals with complex masses [Denner, Dittmaier (2010)]
- Rescue system based on quad-precision CUTTOOLS [Ossola, Papadopoulos, Pittau (2008)]
 - Scalar integrals from ONELOOP [van Hameren, Papadopoulos, Pittau (2009); van Hameren (2010)]

2-loop amplitudes from analytic results

- Drell–Yan-like amplitudes from [Matsuura, van der Marck, van Neerven (1989)]
- $V\gamma$ helicity amplitudes from [Gehrman, Tancredi (2011)], using TDHPL [Gehrman, Remiddi (2001)]
- On-shell VV amplitudes from private code [von Manteuffel, Tancredi (2014)], using GiNAC (applied in [Cascioli et al. (2014); Gehrman et al. (2014); Grazzini, SK, Rathlev, Wiesemann (2015)])
- Off-shell helicity VV' amplitudes from VVAMP [Gehrman, von Manteuffel, Tancredi (2015)], using GiNAC [Bauer, Frink, Kreckel (2002); Vollinga, Weinzierl (2005)]
(independent calculation by [Caola, Henn, Melnikov, Smirnov, Smirnov (2014)])

Idea of the q_T subtraction method for (N)NLO cross sections

Consider the production of a **colourless final state F** via $q\bar{q} \rightarrow F$ or $gg \rightarrow F$:

$$d\sigma_F^{(N)\text{NLO}} \Big|_{q_T \neq 0} = d\sigma_{F+\text{jet}}^{(N)\text{LO}},$$

where q_T refers to the **transverse momentum of the colourless system F** . [Catani, Grazzini (2007)]

$d\sigma_F^{(N)\text{NLO}} \Big|_{q_T \neq 0}$ is singular for $q_T \rightarrow 0$, but the **limiting behaviour is known** from **transverse-momentum resummation**. [Bozzi, Catani, de Florian, Grazzini (2006)]

- Define a **universal counterterm Σ** with the **complementary $q_T \rightarrow 0$ behaviour**, $d\sigma^{\text{CT}} = \Sigma(q_T/Q) \otimes d\sigma^{\text{LO}}$, where Q is the invariant mass of the colourless system F .
- Add the $q_T = 0$ piece with the **hard-virtual coefficient \mathcal{H}_F** , which is derived from the 1-(2-)loop amplitudes at (N)NLO, and also compensates for the subtraction of Σ .

↪ **Full result for (N)NLO cross section**

$$d\sigma_F^{(N)\text{NLO}} = \mathcal{H}_F^{(N)\text{NLO}} \otimes d\sigma^{\text{LO}} + \left[d\sigma_{F+\text{jet}}^{(N)\text{LO}} - \Sigma^{(N)\text{NLO}} \otimes d\sigma^{\text{LO}} \right]_{\text{cut}_{q_T} \rightarrow 0}$$

Ingredients of the q_T subtraction method

$$d\sigma_F^{(N)\text{NLO}} = \mathcal{H}_F^{(N)\text{NLO}} \otimes d\sigma^{\text{LO}} + \left[d\sigma_{F+\text{jet}}^{(N)\text{LO}} - \Sigma^{(N)\text{NLO}} \otimes d\sigma^{\text{LO}} \right]_{\text{cut } q_T \rightarrow 0}$$

- The hard-virtual coefficient \mathcal{H}_F ,

$$\mathcal{H}_F = \underbrace{1}_{\text{tree-level amplitude}} + \underbrace{\left(\frac{\alpha_S}{\pi}\right) \mathcal{H}^{F(1)}}_{\text{contains (finite) 1-loop amplitude}} + \underbrace{\left(\frac{\alpha_S}{\pi}\right)^2 \mathcal{H}^{F(2)}}_{\text{contains (finite) 2-loop amplitude}} + \dots,$$

is known up to 2-loop order by means of a process-independent extraction procedure, starting from the all-order virtual amplitude of the specific process.

[Catani, Cieri, de Florian, Ferrera, Grazzini (2013)]

- The counterterm $\Sigma(q_T/Q)$,

$$\Sigma(q_T/Q) = \left(\frac{\alpha_S}{\pi}\right) \Sigma^{(1)}(q_T/Q) + \left(\frac{\alpha_S}{\pi}\right)^2 \Sigma^{(2)}(q_T/Q) + \dots,$$

is universal (differs for $q\bar{q} \rightarrow F$ and $gg \rightarrow F$, trivial process dependence), and the coefficients are known (up to 2-loop order). [Bozzi, Catani, de Florian, Grazzini (2006)]

- The real-emission contribution $d\sigma_{F+\text{jet}}^{\text{NLO}}$ can be treated by any local NLO subtraction technique, e.g. by conventional dipole subtraction. [Catani, Seymour (1993)]

Numerical realization of the calculation

**Realized within the fully automated NLO (QCD+EW) Monte Carlo framework
MUNICH (MUlti-chaNnel Integrator at Swiss (CH) precision) [SK]**

- Applicable for arbitrary Standard Model processes (including partonic bookkeeping).
- Phase-space integration by highly efficient multi-channel Monte Carlo techniques
→ Additional MC channels based on dipole kinematics constructed at runtime.
- OPENLOOPS interface, automatized implementation of dipole subtraction, etc.
- Simultaneous calculation for different scale choices and variations.

Extension to automated (q_T subtraction) NNLO QCD framework [Grazzini, SK, Rathlev]

- Process-independent construction of $\text{cut}_{q_T/q}$ -dependent counterterms $\Sigma^{(1,2)}$.
- Process-independent extraction procedure for hard coefficients $\mathcal{H}^{(1,2)}$.
- Importance sampling performed on top of multi-channel approach
→ improved efficiency and reliability in particular for low $\text{cut}_{q_T/q}$ values.
- Simultaneous evaluation of observables for different values of the regulator $\text{cut}_{q_T/q}$
→ allows for monitoring of $\text{cut}_{q_T/q}$ and for extrapolation $\text{cut}_{q_T/q} \rightarrow 0$.

NLO QCD cross section via dipole subtraction

Schematic formula for the NLO cross section with dipoles [Catani, Seymour (1993)]

$$\begin{aligned}
 \delta\sigma^{\text{NLO}} &= \underbrace{\int_{m+1} d\sigma^R}_{\text{real corrections}} + \underbrace{\int_m d\sigma^V}_{\text{virtual corrections}} + \underbrace{\int_0^1 dz \int_m d\sigma^C}_{\text{collinear-subtraction counterterm}} - \int_{m+1} d\sigma^A + \int_{m+1} d\sigma^A, \\
 d\sigma^A &= \sum_{\text{dipoles}} d\sigma^B \otimes dV_{\text{dipole}} \\
 &= \int_{m+1} \left[d\sigma^R - d\sigma^A \right]_{\epsilon=0} \Rightarrow \delta\sigma^{\text{RA}} \\
 &\quad + \int_m \left[d\sigma^V + \sum_{\text{dipoles}} d\sigma^B \otimes V_{\text{dipole}}(1) \right]_{\epsilon=0} \Rightarrow \delta\sigma^{\text{VA}} \\
 &\quad + \int_0^1 dz \int_m \left[d\sigma^C + \sum_{\text{dipoles}} \int_1^z d\sigma^B(z) \otimes [dV_{\text{dipole}}(z)]_+ \right]_{\epsilon=0} \Rightarrow \delta\sigma^{\text{CA}}
 \end{aligned}$$

$$dV_{\text{dipole}}(z) = [dV_{\text{dipole}}(z)]_+ + dV_{\text{dipole}}(1)\delta(1-z)$$

→ Local subtraction terms (Catani–Seymour dipole terms) allow for mediation of infrared (soft and collinear) divergences between the different phase spaces.

NLO QCD cross section via q_T subtraction

Schematic formula for the NLO cross section via q_T subtraction [Catani, Grazzini (2007)]

$$\begin{aligned}
 \delta\sigma^{\text{NLO}} &= \underbrace{\int_{m+1} d\sigma^R}_{\text{real}} + \underbrace{\int_m d\sigma^V}_{\text{virtual}} + \underbrace{\int_0^1 dz \int_m d\sigma^C}_{\text{collinear}} \\
 &= \int_{m+1} d\sigma^R \Big|_{q_T/q > \text{cut}_{q_T/q}} \quad \Rightarrow \text{finite, but depends on cut}_{q_T/q} \\
 &\quad + \underbrace{\int_{m+1} d\sigma^R \Big|_{q_T/q \leq \text{cut}_{q_T/q}}}_{\text{approximated by results known from } q_T \text{ resummation}} + \underbrace{\int_m d\sigma^V + \int_0^1 dz \int_m d\sigma^C}_{\text{identified with corresponding terms in } q_T \text{ resummation}} \\
 &\approx \int_{m+1} d\sigma^R \Big|_{q_T/q > \text{cut}_{q_T/q}} + \frac{\alpha_S}{\pi} \mathcal{H}^{F(1)} \otimes \sigma_{\text{LO}} \quad \left\{ \begin{array}{l} \bullet \text{ no cut}_{q_T/q} \text{ dependence,} \\ \bullet \text{ contains (finite) 1-loop part.} \end{array} \right. \\
 &\quad - \frac{\alpha_S}{\pi} \int_{\text{cut}_{q_T/q}}^\infty d(q_T/q) \Sigma^{(1)}(q_T/q) \otimes \sigma_{\text{LO}} \quad \left\{ \begin{array}{l} \bullet \text{ cancels cut}_{q_T/q} \text{ dependence,} \\ \bullet \text{ assigned to Born phase-space.} \end{array} \right.
 \end{aligned}$$

NNLO QCD cross section via q_T subtraction

Schematic formula for the NNLO cross section

$$\delta\sigma^{\text{NNLO}} = \underbrace{\int_{m+2} d\sigma^{RR} + \int_{m+1} d\sigma^{RV} + \int_0^1 dz \int_{m+1} d\sigma^{RC}}_{\text{double-real}} + \underbrace{\int_m d\sigma^{VV} + \int_0^1 dz \int_m d\sigma^{VC} + \int_0^1 dz_1 \int_0^1 dz_2 \int_m d\sigma^{CC}}_{\text{double-virtual}} \\ = \sigma_{F+\text{jet}}^{\text{NLO}} \Rightarrow \begin{array}{l} \text{at } q_T \neq 0 \text{ calculable via NLO subtraction,} \\ \text{but divergent for } q_T \rightarrow 0 \Rightarrow \text{cut}_{q_T/q} \end{array}$$

$$= \sigma_{F+\text{jet}}^{\text{NLO}} \Big|_{q_T/q > \text{cut}_{q_T/q}} + \underbrace{\sigma_{F+\text{jet}}^{\text{NLO}} \Big|_{q_T/q \leq \text{cut}_{q_T/q}} + \int_m d\sigma^{VV} + \int_0^1 dz \int_m d\sigma^{VC} + \int_0^1 dz_1 \int_0^1 dz_2 \int_m d\sigma^{CC}}_{\begin{array}{l} \text{approximated by results known} \\ \text{from } q_T \text{ resummation} \end{array} \quad \begin{array}{l} \text{identified with corresponding terms} \\ \text{in } q_T \text{ resummation} \end{array}}$$

NNLO QCD cross section via q_T subtraction

Schematic formula for the NNLO cross section

$$\delta\sigma^{\text{NNLO}} = \underbrace{\left[\int_{m+2} d\sigma^{RRA} + \int_{m+1} d\sigma^{RVA} + \int_0^1 dz \int_{m+1} d\sigma^{RCA} \right]}_{= \sigma_{F+jet}^{\text{NLO}}} \Big|_{q_T/q > \text{cut}_{q_T/q}} \Rightarrow \text{finite, but depends on } \text{cut}_{q_T/q}$$

$$- \left(\frac{\alpha_S}{\pi} \right)^2 \int_{\text{cut}_{q_T/q}}^\infty d(q_T/q) \Sigma^{(2)}(q_T/q) \otimes \sigma_{\text{LO}} \quad \left\{ \begin{array}{l} \bullet \text{ cancels cut}_{q_T/q} \text{ dependence,} \\ \bullet \text{ contains (finite) 1-loop part,} \\ \bullet \text{ assigned to Born phase-space.} \end{array} \right.$$

$$+ \left(\frac{\alpha_S}{\pi} \right)^2 \mathcal{H}^{(2)} \otimes \sigma_{\text{LO}} \quad \left\{ \begin{array}{l} \bullet \text{ no cut}_{q_T/q} \text{ dependence,} \\ \bullet \text{ contains (finite) 2-loop part.} \end{array} \right.$$

All relevant ingredients from q_T resummation ($\mathcal{H}^{(i)}$, $\Sigma^{(i)}(q_T/q)$ for $i \leq 2$) are known.

↪ Direct implementation into a Monte Carlo integrator feasible.

NNLO QCD results for pp ($\rightarrow V\gamma$) $\rightarrow \ell\ell\gamma/\nu\nu\gamma/\ell\nu\gamma + X$

$$\text{pp } (\rightarrow Z\gamma) \rightarrow \ell^- \ell^+ \gamma + X$$

$$\text{pp } (\rightarrow Z\gamma) \rightarrow \nu_\ell \bar{\nu}_\ell \gamma + X$$

$$\text{pp } (\rightarrow W^+\gamma) \rightarrow \ell^+ \nu_\ell \gamma + X$$

$$\text{pp } (\rightarrow W^-\gamma) \rightarrow \ell^- \bar{\nu}_\ell \gamma + X$$

Setup for pp ($\rightarrow Z\gamma$) $\rightarrow \ell\ell\gamma + X$

Setup adapted to the ATLAS analysis @ 7 TeV

[ATLAS collaboration (2013)]

Leptons

$$p_T^\ell > 25 \text{ GeV}$$

$$|\eta^\ell| < 2.47$$

Photon

$p_T^\gamma > 15 \text{ GeV}$ (soft p_T^γ cut) or $p_T^\gamma > 40 \text{ GeV}$ (hard p_T^γ cut)

$$|\eta^\gamma| < 2.37$$

Frixione isolation with $\epsilon_\gamma = 0.5$, $R = 0.4$, $n = 1$

Jets

anti- k_T algorithm with $D = 0.4$

$$p_T^{\text{jet}} > 30 \text{ GeV}$$

$$|\eta^{\text{jet}}| < 4.4$$

$N_{\text{jet}} \geq 0$ (inclusive) or $N_{\text{jet}} = 0$ (exclusive)

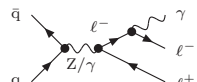
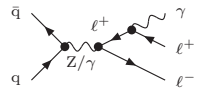
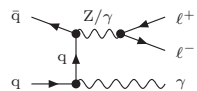
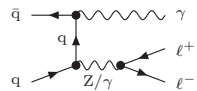
Separation

$$m_{\ell\ell} > 40 \text{ GeV}$$

$$\Delta R(\ell, \gamma) > 0.7$$

$$\Delta R(\ell/\gamma, \text{jet}) > 0.3$$

LO diagrams



Setup for pp ($\rightarrow W\gamma$) $\rightarrow \ell\nu\gamma + X$

Setup adapted to the ATLAS analysis @ 7 TeV

[ATLAS collaboration (2013)]

Lepton

$$p_T^\ell > 25 \text{ GeV}$$

$$|\eta| < 2.47$$

Neutrino

$$p_T^\nu > 35 \text{ GeV}$$

Photon

$p_T^\gamma > 15 \text{ GeV}$ (soft p_T^γ cut) or $p_T^\gamma > 40 \text{ GeV}$ (hard p_T^γ cut)

$$|\eta^\gamma| < 2.37$$

Frixione isolation with $\varepsilon_\gamma = 0.5$, $R = 0.4$, $n = 1$

Jets

anti- k_T algorithm with $D = 0.4$

$$p_T^{\text{jet}} > 30 \text{ GeV}$$

$$|\eta^{\text{jet}}| < 4.4$$

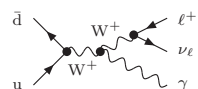
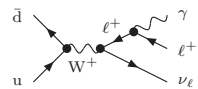
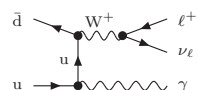
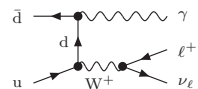
$N_{\text{jet}} \geq 0$ (inclusive) or $N_{\text{jet}} = 0$ (exclusive)

Separation

$$\Delta R(\ell, \gamma) > 0.7$$

$$\Delta R(\ell/\gamma, \text{jet}) > 0.3$$

LO diagrams



Setup for pp ($\rightarrow Z\gamma$) $\rightarrow \nu\nu\gamma + X$

Setup adapted to the ATLAS analysis @ 7 TeV

[ATLAS collaboration (2013)]

Neutrinos

$$p_T^{\nu\bar{\nu}} > 90 \text{ GeV}$$

Photon

$$p_T^\gamma > 100 \text{ GeV}$$

$$|\eta^\gamma| < 2.37$$

Frixione isolation with $\varepsilon_\gamma = 0.5$, $R = 0.4$, $n = 1$

Jets

$$p_T^{\text{jet}} > 30 \text{ GeV}$$

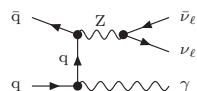
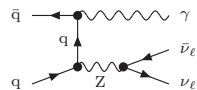
$$|\eta^{\text{jet}}| < 4.4$$

$N_{\text{jet}} \geq 0$ (inclusive) or $N_{\text{jet}} = 0$ (exclusive)

Separation

$$\Delta R(\gamma, \text{jet}) > 0.3$$

LO diagrams



Photon isolation

Two contributions to photon production

- Direct production in the hard process,
- Non-perturbative fragmentation of a hard parton.

Different approaches to define isolated photons

- Naive ansatz: forbid any partons inside a fixed cone around the photon.
 \hookrightarrow Not infrared safe beyond LO QCD as soft gluons inside the cone are forbidden.
- Hard cone isolation (experimentally preferred)

$$\sum_{\delta' < \delta_0} E_{\text{had},T}(\delta') \leq \varepsilon_\gamma E_{\gamma,T}, \quad \delta_{i\gamma} = \sqrt{(\eta_i - \eta_\gamma)^2 + (\phi_i - \phi_\gamma)^2}$$

\hookrightarrow Only infrared safe if combined with fragmentation contribution
 (due to quark–photon collinear singularity).

- Smooth cone isolation [Frixione (1998)]

$$\sum_{\delta' < \delta} E_{\text{had},T}(\delta') \leq \varepsilon_\gamma E_{\gamma,T} \left(\frac{1 - \cos(\delta)}{1 - \cos(\delta_0)} \right)^n \quad \forall \quad \delta \leq \delta_0$$

\hookrightarrow Smooth cone isolation eliminates fragmentation contribution completely.

Fiducial cross sections for pp ($\rightarrow V\gamma$) $\rightarrow \ell\ell\gamma/\ell\nu\gamma/\nu\nu\gamma + X$

Setup adapted to the ATLAS analysis @ 7 TeV [ATLAS collaboration (2013)]

| process | p_T^γ , cut | N_{jet} | $\sigma_{\text{LO}} [\text{pb}]$ | $\sigma_{\text{NLO}} [\text{pb}]$ | $\sigma_{\text{NNLO}} [\text{pb}]$ | $\sigma_{\text{ATLAS}} [\text{pb}]$ | $\frac{\sigma_{\text{NLO}}}{\sigma_{\text{LO}}}$ | $\frac{\sigma_{\text{NNLO}}}{\sigma_{\text{NLO}}}$ |
|---|--------------------|------------------|----------------------------------|-----------------------------------|------------------------------------|---|--|--|
| $Z\gamma$ $\rightarrow \ell\ell\gamma$ | soft | ≥ 0 | 0.8149 $^{+8.0\%}_{-9.3\%}$ | 1.222 $^{+4.2\%}_{-5.3\%}$ | 1.320 $^{+1.3\%}_{-2.3\%}$ | 1.31 $^{+0.02 \text{ (stat)}}_{\pm 0.11 \text{ (syst)}}^{+0.05 \text{ (lumi)}}$ | +50% | +8% |
| | | = 0 | | 1.031 $^{+2.7\%}_{-4.3\%}$ | 1.059 $^{+0.7\%}_{-1.4\%}$ | 1.05 $^{+0.02 \text{ (stat)}}_{\pm 0.10 \text{ (syst)}}^{+0.04 \text{ (lumi)}}$ | +27% | +3% |
| | hard | ≥ 0 | 0.0736 $^{+3.4\%}_{-4.5\%}$ | 0.1320 $^{+4.2\%}_{-4.0\%}$ | 0.1543 $^{+3.1\%}_{-2.8\%}$ | | +79% | +17% |
| $Z\gamma$ $\rightarrow \nu\nu\gamma$ | | ≥ 0 | 0.0788 $^{+0.3\%}_{-0.9\%}$ | 0.1237 $^{+4.1\%}_{-3.1\%}$ | 0.1380 $^{+2.5\%}_{-2.3\%}$ | 0.133 $^{+0.013 \text{ (stat)}}_{\pm 0.020 \text{ (syst)}}^{+0.005 \text{ (lumi)}}$ | +57% | +12% |
| | | = 0 | | 0.0881 $^{+1.2\%}_{-1.3\%}$ | 0.0866 $^{+1.0\%}_{-0.9\%}$ | 0.116 $^{+0.010 \text{ (stat)}}_{\pm 0.013 \text{ (syst)}}^{+0.004 \text{ (lumi)}}$ | +12% | -2% |
| $W\gamma$ $\rightarrow \ell\nu\gamma$ | soft | ≥ 0 | 0.8726 $^{+6.8\%}_{-8.1\%}$ | 2.058 $^{+6.8\%}_{-6.8\%}$ | 2.453 $^{+4.1\%}_{-4.1\%}$ | 2.77 $^{+0.03 \text{ (stat)}}_{\pm 0.33 \text{ (syst)}}^{+0.14 \text{ (lumi)}}$ | +136% | +19% |
| | | = 0 | | 1.395 $^{+5.2\%}_{-5.8\%}$ | 1.493 $^{+1.7\%}_{-2.7\%}$ | 1.76 $^{+0.03 \text{ (stat)}}_{\pm 0.21 \text{ (syst)}}^{+0.08 \text{ (lumi)}}$ | +60% | +7% |
| | hard | ≥ 0 | 0.1158 $^{+2.6\%}_{-3.7\%}$ | 0.3959 $^{+9.0\%}_{-7.3\%}$ | 0.4971 $^{+5.3\%}_{-4.7\%}$ | | +242% | +26% |

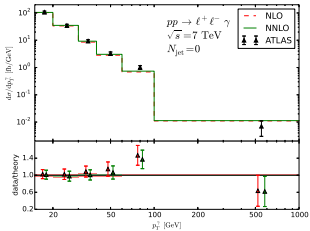
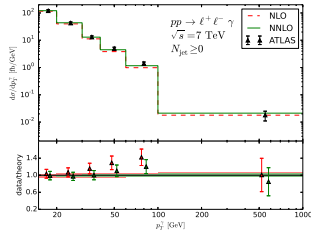
- Loop-induced gg contributions in $Z\gamma$ turn out to be very small (< 15% of NNLO).
- Larger K factors in $W\gamma$ than in $Z\gamma$ can be explained by breaking of radiation zero.
- Larger K factors in hard than in soft setups due to implicit phase-space restrictions.

p_T^γ distributions for pp ($\rightarrow Z\gamma/W\gamma$) $\rightarrow \ell\ell\gamma/\ell\nu\gamma + X$

pp ($\rightarrow Z\gamma$) $\rightarrow \ell\ell\gamma + X$

$N_{\text{jet}} \geq 0$ (left)

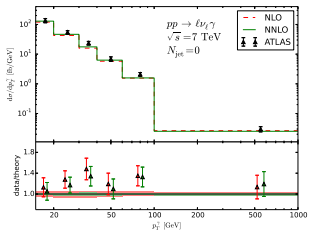
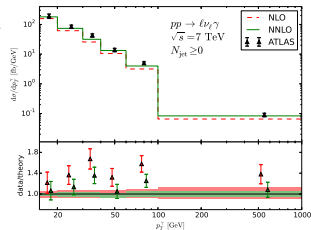
$N_{\text{jet}} = 0$ (right)



pp ($\rightarrow W\gamma$) $\rightarrow \ell\nu\gamma + X$

$N_{\text{jet}} \geq 0$ (left)

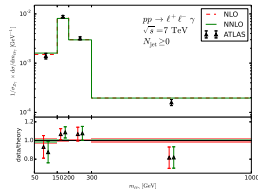
$N_{\text{jet}} = 0$ (right)



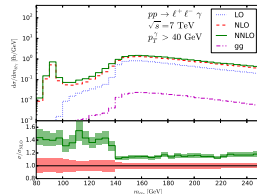
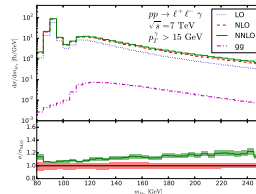
- Agreement between data and theory is significantly improved when including NNLO corrections as compared to NLO prediction, in particular without jet veto.
- No NLO EW corrections included, which become large and negative for higher p_T 's.
[Denner, Dittmaier, Hecht, Pasold (2014 & 2015)]

Invariant/transverse mass distributions for $pp \rightarrow \ell\ell\gamma/\ell\nu\gamma/\nu\nu\gamma + X$

$pp (\rightarrow Z\gamma) \rightarrow \ell\ell\gamma + X$

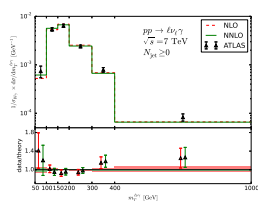


Distribution in the invariant mass $m_{\ell\ell\gamma}$

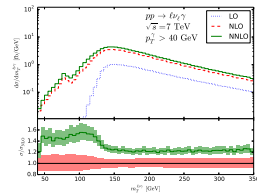
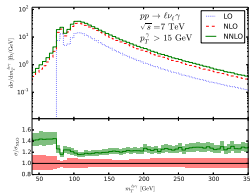


- Implicit LO phase-space restrictions: $m_{\ell\ell\gamma} \approx 66$ GeV (soft) vs. $m_{\ell\ell\gamma} \approx 97$ GeV (hard)

$pp (\rightarrow W\gamma) \rightarrow \ell\nu\gamma + X$



Distribution in the transverse mass $m_T^{\ell\nu\gamma}$



- Implicit LO phase-space restrictions: $m_T^{\ell\nu\gamma} \approx 75$ GeV (soft) vs. $m_T^{\ell\nu\gamma} \approx 100$ GeV (hard)

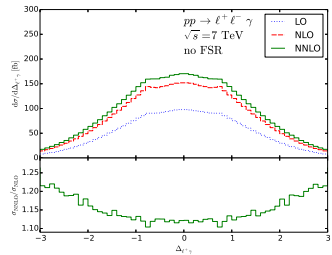
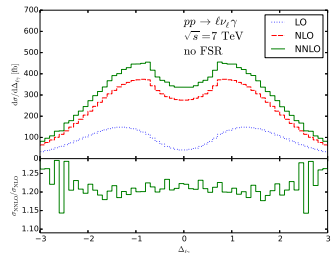
Comparison between $Z\gamma$ and $W\gamma$ results

Considerably larger K factors in $W\gamma$ than in $Z\gamma$

| process | $p_{T,\text{cut}}^\gamma$ | N_{jet} | $\frac{\sigma_{\text{NLO}}}{\sigma_{\text{LO}}}$ | $\frac{\sigma_{\text{NNLO}}}{\sigma_{\text{NLO}}}$ |
|-----------|---------------------------|-------------------------|--|--|
| $Z\gamma$ | soft | $N_{\text{jet}} \geq 0$ | +50% | +8% |
| | | | +136% | +19% |
| $W\gamma$ | soft | $N_{\text{jet}} = 0$ | +27% | +3% |
| | | | +60% | +7% |
| $Z\gamma$ | hard | $N_{\text{jet}} \geq 0$ | +79% | +17% |
| | | | +242% | +26% |

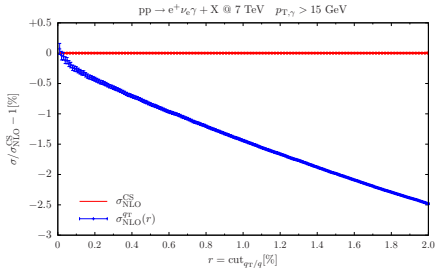
Explanation: **Breaking of radiation zero beyond LO**

- $u\bar{d}/d\bar{u} \rightarrow W^\pm\gamma$ amplitudes vanish at $\cos\theta_{q\gamma, \text{CMS}} = \mp 1/3$. [Mikaelian/Samuel/Sahdev (1979)]
 - Radiation zero leads to a dip at $\Delta y_{\ell\gamma} = 0$ in pp collisions. [Baur/Errede/Landsberg (1994)]
- ↪ Dip filled by higher-order corrections.

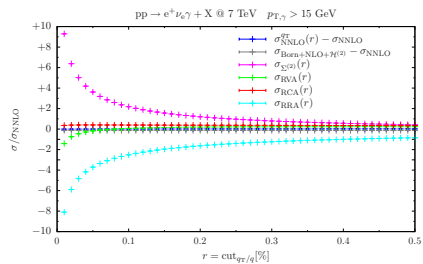
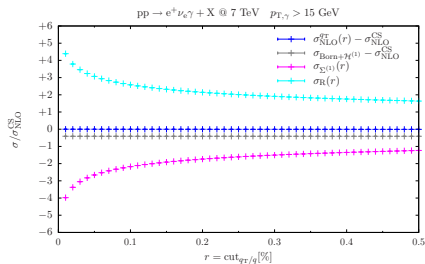
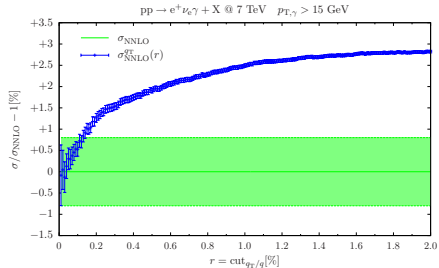


Numerical stability and dependence on cut $_{q_T/q}$

q_T subtraction at NLO



q_T subtraction at NNLO



NNLO QCD results for $\text{pp} (\rightarrow W^\pm Z) \rightarrow 3\ell\nu + X$

$$\text{pp} \rightarrow W^+ Z + X$$

$$\text{pp} \rightarrow W^- Z + X$$

$$\text{pp } (\rightarrow W^+ Z) \rightarrow \ell^- \ell^+ \ell'^+ \nu_{\ell'} + X$$

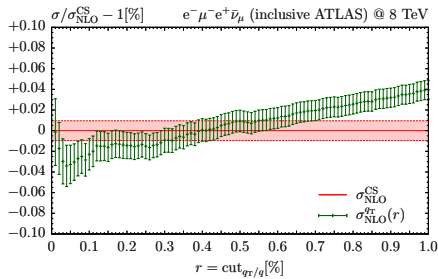
$$\text{pp } (\rightarrow W^- Z) \rightarrow \ell^- \ell'^- \ell^+ \bar{\nu}_{\ell'} + X$$

$$\text{pp } (\rightarrow W^+ Z) \rightarrow \ell^- \ell^+ \ell^+ \nu_\ell + X$$

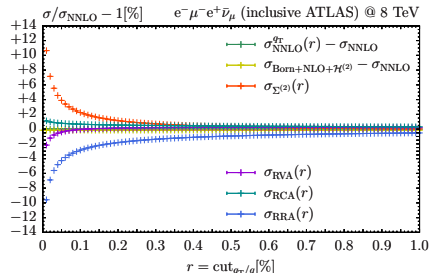
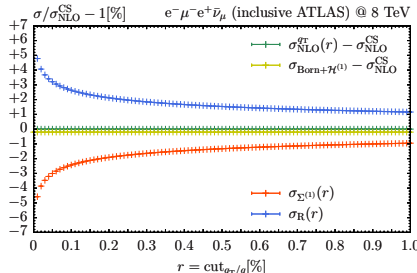
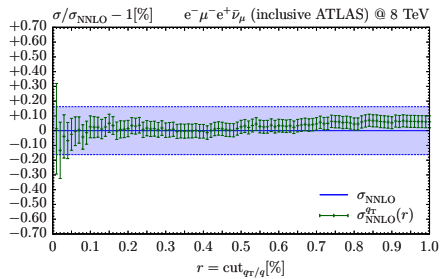
$$\text{pp } (\rightarrow W^- Z) \rightarrow \ell^- \ell^- \ell^+ \bar{\nu}_\ell + X$$

Dependence on cut $_{q_T/q}$ – inclusive ATLAS @ 8 TeV

q_T subtraction at NLO



q_T subtraction at NNLO



NNLO QCD results for pp ($\rightarrow W^+W^-$) $\rightarrow 2\ell 2\nu + X$

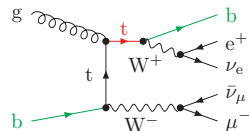
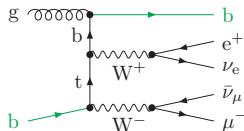
$$pp \rightarrow W^+ W^- + X$$

$$pp (\rightarrow W^+ W^-) \rightarrow \ell^- \ell'^+ \nu_{\ell'} \bar{\nu}_{\ell} + X$$

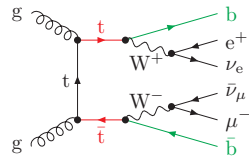
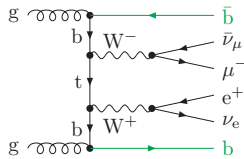
$$pp (\rightarrow W^+ W^- / ZZ) \rightarrow \ell^- \ell^+ \nu_{\ell} \bar{\nu}_{\ell} + X$$

Definition of top-contamination free WW cross section

- Non-trivial in 5FNS (massless b's \rightarrow WW and WWb \bar{b} connected by IR structure)
- Single-top production enters at NLO.



- Top-pair production enters at NNLO.



→ Huge "higher-order corrections" result from top-resonance contamination in 5FNS
(cross-section enhancement of 30%/400% at NLO/NNLO for $\sqrt{s} = 8$ TeV).

- Straightforward in 4FNS (massive b's \rightarrow WWb \bar{b} finite and can be split off)

Extrapolation in top width to isolate WW contributions

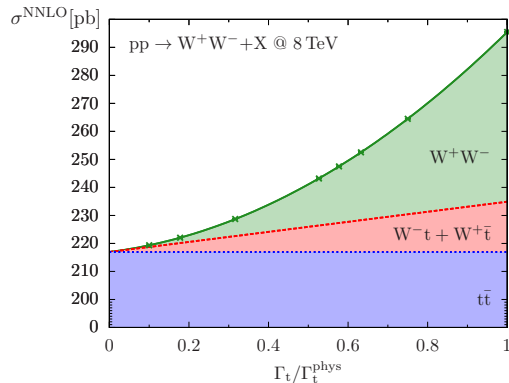
Γ_t -dependence of NNLO cross section can be used to isolate the different processes

- Exploit the Γ_t dependence of the genuine WW, tW, and t \bar{t} contributions,

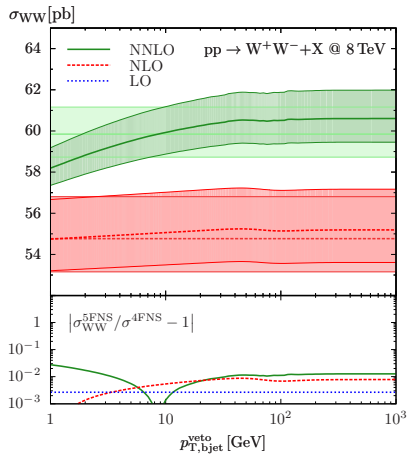
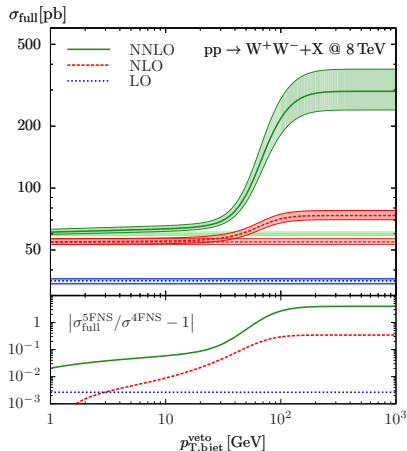
$$\sigma_{WW} \propto 1, \quad \sigma_{tW} \propto 1/\Gamma_t, \quad \sigma_{t\bar{t}} \propto 1/\Gamma_t^2,$$

and treat Γ_t as technical parameter to approach the $\Gamma_t \rightarrow 0$ limit.

- ↪ Parabolic fit of the $(\Gamma_t/\Gamma_t^{\text{phys}})^2$ -rescaled cross section delivers σ_{WW} , σ_{tW} , $\sigma_{t\bar{t}}$.



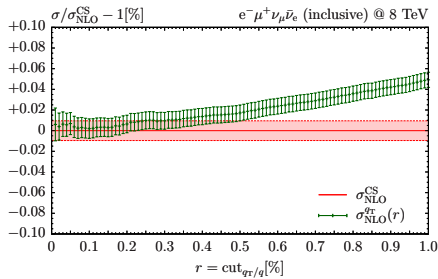
Comparison between 4FNS and 5FNS WW cross sections



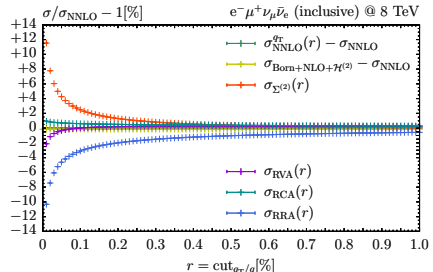
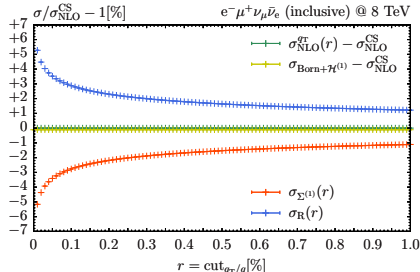
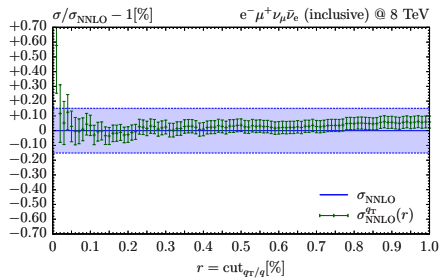
- About 15% of enhancement remain at NNLO for “physical” $p_{\text{T},\text{bjet}}^{\text{veto}} \approx 30 \text{ GeV}$.
- The limit $p_{\text{T},\text{bjet}}^{\text{veto}} \rightarrow 0 \text{ GeV}$ cannot be directly accessed (Infrared divergent in 5FNS).
- Extrapolation gives $\approx 1\text{-}2\%$ agreement between 4FNS and 5FNS for $p_{\text{T},\text{bjet}}^{\text{veto}} \rightarrow \infty$.

Dependence on cut $_{q_T/q}$ – inclusive @ 8 TeV

q_T subtraction at NLO

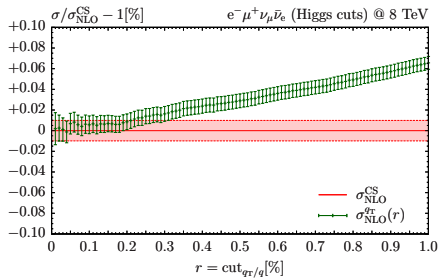


q_T subtraction at NNLO

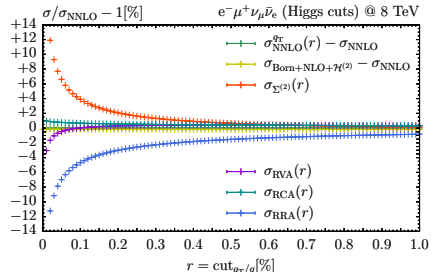
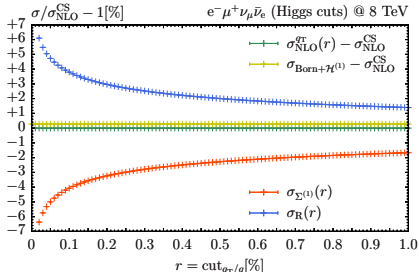
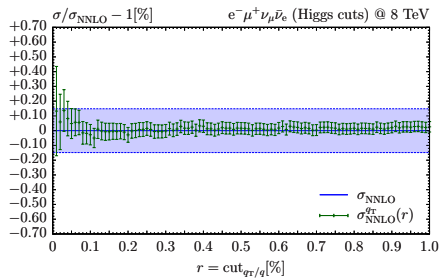


Dependence on cut $_{q_T/q}$ – Higgs @ 8 TeV

q_T subtraction at NLO



q_T subtraction at NNLO



NNLO QCD results for pp ($\rightarrow ZZ$) $\rightarrow 4\ell + X$

pp $\rightarrow Z Z + X$

pp ($\rightarrow ZZ$) $\rightarrow \ell^- \ell^+ \ell'^- \ell'^+ + X$

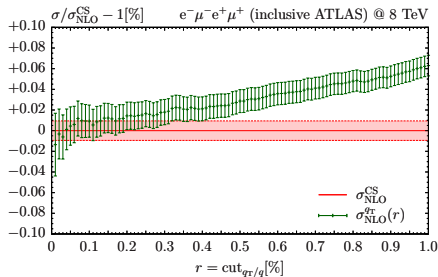
pp ($\rightarrow ZZ$) $\rightarrow \ell^- \ell^+ \ell^- \ell^+ + X$

pp ($\rightarrow ZZ$) $\rightarrow \ell^- \ell^+ \nu_{\ell'} \bar{\nu}_{\ell'} + X$

pp ($\rightarrow W^+W^-/ZZ$) $\rightarrow \ell^- \ell^+ \nu_\ell \bar{\nu}_\ell + X$

Dependence on cut $_{q_T/q}$ – inclusive ATLAS @ 8 TeV

q_T subtraction at NLO



q_T subtraction at NNLO

